Marine Pollution Bulletin 207 (2024) 116886

Contents lists available at ScienceDirect

Marine Pollution Bulletin

journal homepage: www.elsevier.com/locate/marpolbul

Investigating the link between the Port of Miami dredging and the onset of the stony coral tissue loss disease epidemics

Thomas Dobbelaere [a,*], Daniel M. Holstein [d], Lewis J. Gramer [b,c], Lucas McEachron [e], Emmanuel Hanert [a,f]

[a] Eath and Life Institute (ELI), UCLouvain, Louvain-la-Neuve, Belgium
[b] Cooperative Institute for Marine and Atmospheric Studies (CIMAS), University of Miami, Miami, FL, USA
[c] Atlantic Oceanographic and Meteorological Laboratory (AOML), NOAA, Miami, FL, USA
[d] Department of Oceanography and Coastal Sciences, College of the Coast and Environment, Louisiana State University, Baton Rouge, LA, USA
[e] Fish and Wildlife Research Institute, Florida Fish and Wildlife Conservation Commission, Saint Petersburg, FL, USA
[f] Institute of Mechanics, Materials and Civil Engineering (IMMC), UCLouvain, Louvain-la-Neuve, Belgium

ARTICLE INFO

Keywords:
Stony coral tissue loss disease
Multiscale coastal modeling
Port of Miami
Sediment plumes
Dredging

ABSTRACT

Since 2014, the stony coral tissue loss disease (SCTLD) has been decimating corals in the Caribbean. Although the trigger of this outbreak remains elusive, evidence suggests waterborne sediment-mediated disease transmission. The outbreak reportedly initiated in September 2014 at a reef site off Virginia Key (VKR), during extensive dredging operations at the Port of Miami. Here we use a high-resolution ocean model to identify the potential driver of the outbreak by simulating the dispersal of dredged sediments, wastewater plumes and disease agents. Our results suggest that VKR could have been impacted by fine sediments produced by dredging operations, especially those involving non-conventional rock-chopping techniques. Wastewater contamination was unlikely. Additionally, our connectivity analysis indicates potential disease transmission from other affected reefs to VKR. Our results therefore suggest that dredging operations might be responsible for the onset of the epidemics. This underscores the need for stricter operational guidelines in future dredging projects.

1. Introduction

Coral reefs, which cover just 0.2 % of the ocean floor, are among the most biologically diverse ecosystems on Earth, supporting over a quarter of all marine species. Their complex calcium carbonate structures not only provide critical habitats for marine life, offering shelter, sustenance, and breeding grounds, but also protect coastal areas against storms and floods (Moberg and Folke, 1999; Spalding and Grenfell, 1997; Rogers et al., 2014; Ferrario et al., 2014; Elliff and Silva, 2017). Despite their ecological and protective roles, coral reefs are experiencing a dramatic decline globally, with approximately 50 % of live coral cover lost since the 1950s due to a combination of global factors like ocean warming and acidification, and local pressures including pollution, overfishing, and unsustainable coastal development (Eddy et al., 2021). Moreover, diseases have become an additional threat, particularly in the Caribbean, where repeated outbreaks have drastically reduced acroporid cover by up to 95 %, driving significant ecological shifts from coral-dominated to algal-dominated reefs (Richardson et al., 1998; Sutherland et al., 2004; Aronson and Precht, 2001; Harvell et al., 2007; Brandt and McManus, 2009).

The latest and most severe of these coral diseases is the stony coral tissue loss disease (SCTLD). It was first detected at a reef site (hereafter referred to as VKR) located off the coast of Virginia Key in September 2014 (Precht et al., 2016) and has since then propagated throughout the Florida Coral Reef (FCR) and across several Caribbean territories (Muller et al., 2020; Dobbelaere et al., 2022b; Kramer et al., 2019; Meiling et al., 2021; Estrada-Saldívar et al., 2021; Heres et al., 2021). Although the etiological agent of SCTLD – whether bacterial or viral – is yet to be determined, hydrodynamic processes are thought to be crucial in spreading the disease agents. This is supported by modeling studies and *ex situ* experiments, which all suggest waterborne transmission (Aeby et al., 2019; Dobbelaere et al., 2020; Eaton et al., 2021; Meiling et al., 2021). Recent studies further indicate that sediments might act as vectors for the disease (Rosales et al., 2020; Studivan et al., 2022).

The first SCTLD observations occurred concurrently with the dredging of the Port of Miami (PoM), which was conducted from

* Corresponding author.
E-mail address: thomas.dobbelaere@uclouvain.be (T. Dobbelaere).

https://doi.org/10.1016/j.marpolbul.2024.116886
Received 21 May 2024; Received in revised form 19 August 2024; Accepted 20 August 2024
Available online 30 August 2024

November 20, 2013, to March 16, 2015. It aimed to accommodate larger post-Panamax class ships by deepening the shipping channel from approximately 12.8 to 15.2 m and widening it at certain bends. This extensive 17-month project involved the removal of about 4.4 million cubic meters of material (NOAA's National Marine Fisheries Service, 2023). Typically, this material was collected on barges and transported to the US Environmental Protection Agency-designated Ocean Dredge Material Disposal Site (ODMDS), located approximately 8.7 km offshore at depths ranging from 120 to 240 m (NOAA's National Marine Fisheries Service, 2023). Certain dredging operations, referred to as "non-conventional", were not covered in the Environmental Impact Statement (EIS). These involved "rock chopping" – a process where the draghead of a Cutterhead Suction Dredge (CSD) grinds or pulverizes rock without suction (U.S. Army Corps of Engineers, 2023). This technique creates "rock flour", a very fine, clay-like material that settles slowly and can disperse over large distances. Most of these non-conventional operations occurred between December 2013 and May 2014 to pre-treat hard rock (see temporal chart in Fig. 1E). The use of rock chopping was estimated to cause up to 33 cm of sediment deposition over 874,121 m^2 of reef around the outer entrance channel (U.S. Army Corps of Engineers, 2023). Further studies highlighted the extensive impact of the dredging, with sediment plumes covering up to 11 km^2 of coral area within 5–10 km from the operations (Barnes et al., 2015) and contributing to the death of over 560,000 coral colonies within 0.5 km of the channel (Cunning et al., 2019).

Sediments released during dredging impact coral biology in several ways (Fabricius, 2005), primarily through increased turbidity and sedimentation (Erftemeijer et al., 2012; Jones et al., 2015). Turbidity from suspended sediments reduces light availability to symbiotic zooxanthellae, which are crucial for coral subsistence as they perform photosynthesis. This reduction in light leads to decreased coral cover and slower growth rates (Kendall Jr et al., 1983; Rogers, 1990; Anthony, 1999; Hennige et al., 2008). Sedimentation can smother or bury coral polyps, severely disrupting their normal functions (Erftemeijer et al., 2012; Jones et al., 2015, 2019). Both sedimentation and turbidity also impair larval recruitment by inhibiting settlement and decreasing larval survival in the water column (Jones et al., 2015). Fine-grained sediments are particularly detrimental as they significantly reduce light penetration (Storlazzi et al., 2015; Fourney and Figueiredo, 2017). Furthermore, these sediments often carry high nutrient loads that can alter the coral microbiome and promote eutrophication, increasing microbial activity and potentially leading to anoxic conditions near coral structures (Rosales et al., 2019; Wittenberg and Hunte, 1992; Weber et al., 2012). Given that dredging releases finer sediments over longer periods than natural events like hurricanes, it poses a greater threat to coral health and reef habitats (Cunning et al., 2019).

While high coral mortality observed during the PoM dredging project could likely be attributed to sediment impacts, Gintert et al. (2019) argue that it was predominantly due to the regional outbreak of SCTLD. They further suggest that this outbreak may have been triggered by wastewater pollution, specifically linking it to a leak from the Miami Central District Municipal Wastewater Treatment Plant (WWTP) off Virginia Key. Although the leak was only reported in 2017 (Staletovich, 2017b), it is possible that the pipe was already leaking in 2014 due to poor maintenance. Although sediments released during dredging have been recognized as potential vectors for SCTLD (Studivan et al., 2022) and known to increase the prevalence of coral diseases (Pollock et al., 2014), the hypothesis that wastewater rather than sediments was the primary conduit for the disease offers a compelling alternative that warrants further investigation. It is also important to note that the first reported signs of the disease followed a major bleaching event, although no significant correlation was found between bleaching and disease (Spadafore et al., 2021). Here, we have simulated both the sediment and wastewater dispersal using a coastal ocean model to simulate the hydrodynamics and transport pathways of contaminants from the dredging site and the wastewater discharge, with sufficient spatial resolution to accurately represent the dynamics at both the dredging and coral reef sites.

In this study, we investigate various transmission scenarios to elucidate the origins of the STCLD outbreak, aiming to identify the pathways through which the disease could have spread to the initially affected sites. Our focus was particularly on the VKR site, believed to be the origin of the outbreak, as well as four nearby sites that also exhibited signs of the disease during the dredging operations (Precht et al., 2016). Initially, we evaluated the impact of sediments dispersed by the Port-Miami Deep Dredge Project (PMDDP) using the multi-scale ocean model SLIM, coupled with a sediment transport model. Subsequently, we modeled the dispersal of pollutant plumes to explore potential contamination from wastewater leaks at the Miami Central Municipal WWTP's discharge pipe. Lastly, given the potential for waterborne transmission of SCTLD (Aeby et al., 2019; Eaton et al., 2021; Meiling et al., 2021), we used a previously validated hydro-epidemiological model to assess the likelihood of disease spread to VKR from reefs affected by non-conventional dredging operations (Dobbelaere et al., 2022b).

2. Materials and methods

Precht et al. (2016) reported the first signs of SCTLD on September 26th, 2014, at a reef site (VKR) near Virginia Key, an island located about one kilometer east of the Port of Miami (PoM, Fig. 1B). The outbreak was first described as white-plague-like disease with extremely high prevalence that affected at least 13 species. In that study, the authors also reported disease occurrences at other neighbouring monitoring sites: Emerald Reef (on December 5th, 2014), Rainbow Reef (on November 4th, 2014) and N. Sunny Isle (on December 6th, 2024). The timing and locations of these observations suggested that the outbreak originated from VKR and propagated both northward and southward. During the 17 months of dredging, 26 permanent monitoring stations were further established within Miami-Dade County (Gintert et al., 2019). No signs of disease were reported at these sites before September 2014, with the possible exception of site HBSC1-CP (see location in Fig. 1B) in May 2014. However, it is unclear whether these were signs of SCTLD or of another coral disease (see Appendix A).

2.1. Sediment plume and deposition

Given the location of the monitoring sites where disease signs were observed during the dredging operations and the northward ocean circulation patterns that predominantly transport sediments in that direction, we considered an area of interest situated between Florida and the Bahamian Banks, and between 25.5°N and 27.5°N (Fig. 1A). We simulated the hydrodynamics with the multiscale ocean model SLIM.[1] This model has already been extensively used and validated in the FCR (Frys et al., 2020; Dobbelaere et al., 2020, 2022a, 2022b). SLIM uses an unstructured mesh whose resolution can be locally increased in order to accurately represent fine-scale flow features. The model resolution was defined by following the same approach as (Dobbelaere et al., 2020). It reaches a resolution of ~100 m over coral reefs and near the PoM to precisely represent the dredged channel (Fig. 1B). The mesh is composed of $\sim 1.76 \times 10^5$ triangles and was generated with the seamsh[2] Python library, which is based on the open-source mesh generator GMSH (Geuzaine and Remacle, 2009). The model was run between October 15, 2013, and September 26, 2014, with a time step of 10 min to cover the whole dredging period prior to the observation of SCTLD at VKR by Precht et al. (2016). The modeled sea surface elevation and currents were exported every hour. Using such a fine mesh resolution, we simulated fine-scale details of the ocean currents, such as the flow

[1] https://www.slim-ocean.be
[2] https://pypi.org/project/seamsh/

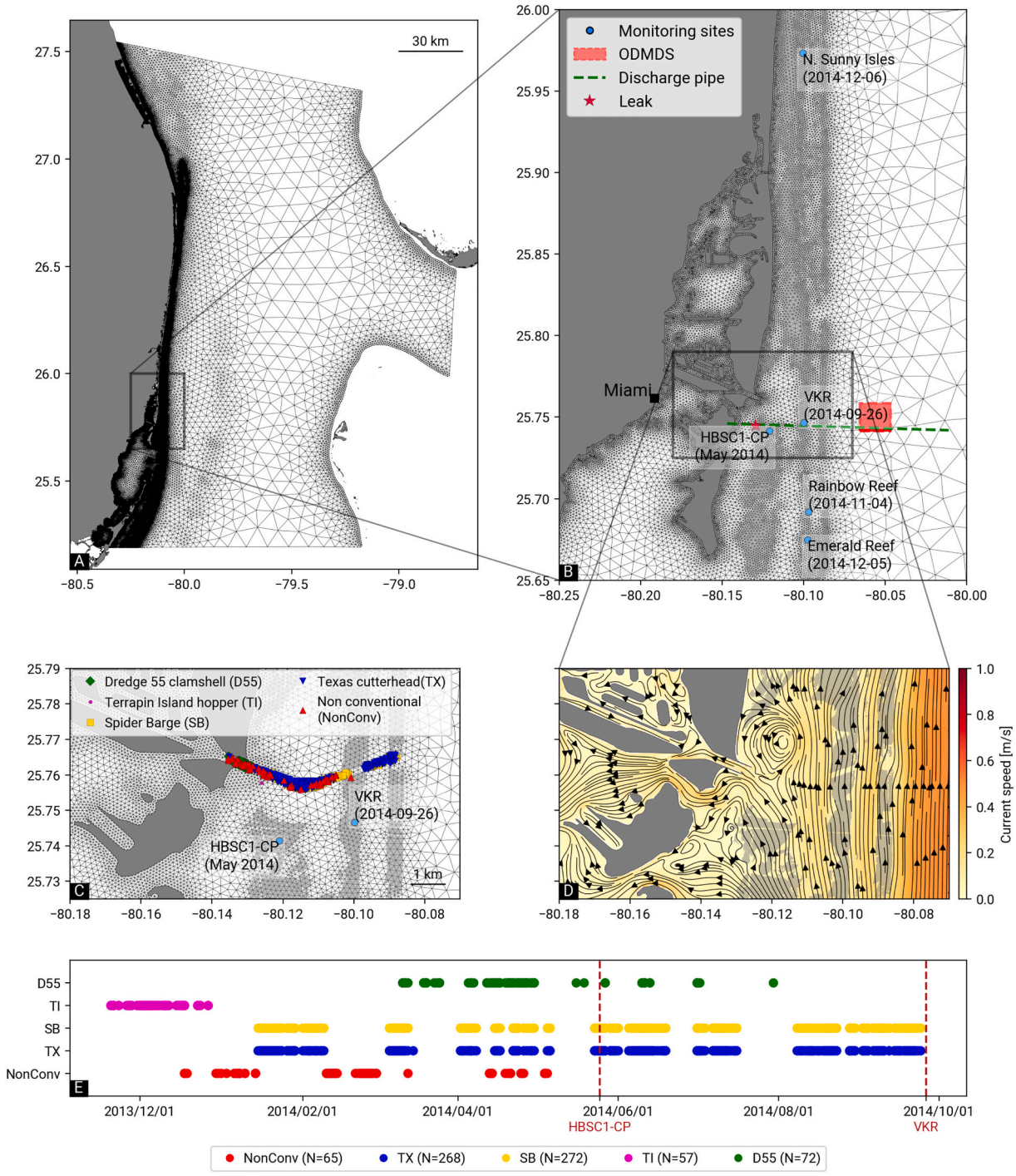

Fig. 1. Model mesh (A) over the whole domain and (B) near the dredged channel. The mesh resolution reaches ~100 m over the reefs (in light gray) and along the coasts (in dark gray). The coral reef monitoring sites are shown by light blue dots. The date of the first reported signs of SCTLD at these sites is given between brackets. The Ocean Dredge Material Disposal Site (ODMDS) is shown in red, the discharge pipe of the Miami Central Municipal WWTP in green, and the pipe's reported leak location is shown by a red star. (C) Close-up view on the dredged channel. The locations of the different types of dredging that took place during the PortMiami expansion are shown by colored markers. (D) Snapshot of the modeled currents in the vicinity of the dredged channel. Small-scale flow features such as the acceleration of currents between reefs and islands are well reproduced by the model.(E) Temporal chart of the simulated period with the temporal distribution of the simulated dredging operations. The dates of the first reported disease signs at HBSC1-CP and VKR sites are shown with dotted dark red vertical lines. The total number of simulated dredging operations (N) is given between brackets for each dredging type. (For interpretation of the references to colour in this figure legend, the reader is referred to the web version of this article.)

acceleration between reefs and islands (Fig. 1D). Atmospheric forcings were obtained from the European Centre for Medium-range Weather Forecasts (ECMWF) ERA-5 dataset and currents were relaxed towards the operational Navy HYbrid Coordinate Ocean Model (HYCOM; Chassignet et al., 2007) following the approach of Dobbelaere et al. (2022a).

The modeled sea surface elevation was validated using tide gauge measurements from the National Data Buoy Center at stations 8722670 and 8723214, which are respectively located at Lake Worth Pier and Virginia Key (see Appendix B).

We then simulated the transport of sediments released by different

dredging operations along the channel with a Lagrangian transport model forced by the simulated currents. Our sediment transport model is inspired by the Particle Transport Model (PTM), developed by the US Army Corps of Engineers (MacDonald et al., 2006). In this model, each particle represents a cluster of sediments, with a certain mass, which undergo a combination of horizontal and vertical motions. The vertical dynamics is mostly driven by gravity, with heavier particles sinking faster. Once they have settled, particles can be resuspended when shear stress exceeds the critical Schields parameter, as expressed by Soulsby et al. (1997). The horizontal motion of the suspended particles is derived from the 2D model velocity by assuming a vertical log profile, hence yielding a quasi-3D approach. Furthermore, to account for the impact of wave-induced sediment motion, these current velocities were combined with surface Stokes drift velocity with Breivik's vertical profile (Breivik et al., 2016). Stokes drift's velocities were downloaded from Copernicus Marine Services's (CMEMS) Ocean Wave Reanalysis dataset (E.U. Copernicus Marine Service Information (CMEMS), 1993–2021). When sediment particles enter the near-bed zone, their horizontal velocity is greatly reduced and sediments are transported with the bed load.

As sediment dispersion is dependent on the grain size, we simulated the dispersal of five sediment classes to represent impacts of fine- to coarse-grained particles: 5–50 μm, 50–100 μm, 100–200 μm, 200–300 μm, and 300–400 μm. We performed a different simulation for each class, with the grain size randomly drawn from a uniform distribution over the corresponding size range, following the methodology of Saint-Amand et al. (2022). The density of each sediment particle was derived from its size using the formula of Hamilton and Bachman (1982). Furthermore, all particles were differentiated based on the type of dredge that produced them. Five types of dredge were considered in our modeling study: Texas cutterhead (TX), non-conventional dredging, *i.e.* TX with suction mechanism turned off (NonConv), Spider Barge (SB), Terrapin Island hopper (TI), and Dredge 55 clamshell (D55). Cutterheads are hydraulic dredges with rotating blades or teeth that pulverize rocks, while clamshells and hoppers respectively remove bottom sediments using bucket-shaped tools and powerful pumps. Spider barges were used in conjunction with TX cutterheads for conventional rock-chopping to transport the dredged material to the ODMDS.

Dredging operations performed during the expansion of PoM were characterized in our dataset by a date, a location and a type of dredge (Fig. 1C). In the absence of information about the exact timing of the dredging, sediment particles were released from the dredging location during a whole day at a rate of 80 particles/h in the model. To account for the motion of spider barges between the dredging and disposal sites, particles were released every 500 m along a straight line joining the dredging location to the ODMDS (see Fig. 1B) for every dredging operation labelled as SB.

We estimated the impact of the simulated sediment plumes on coral reefs by computing the turbidity and sedimentation generated by each type of dredging operations. Turbidity was derived from the concentration of suspended sediment particles. It is computed by counting the number of suspended virtual particles within the cells of a regular 200 m × 200 m grid covering the entire computational domain. The modeled plumes were then compared with daily plume observations derived from satellite imagery by Cunning et al. (2019)[3] following the methods of Barnes et al. (2015) at sites located within 15 km of the dredged channel. As in these two studies, we computed the simulated plume frequency by dividing the number of days during which sediment plumes occurred by the total number of simulated days for all grid cells. Sedimentation was quantified by computing the cumulated concentration of settled particles within the same grid as for turbidity. This cumulated concentration was normalized by the total numbers of simulated time steps and released particles. The normalized sedimentation indicator gives the averaged fraction of the total mass of particles released that settled in each grid cell by unit of area during the simulation. Although its integral is ≤ 1, this indicator is similar to a probability density giving the probability of presence of deposited sediments per unit area over the whole simulated period. By construction, high values of this indicator indicate larger sediment deposition over a longer cumulated time in the simulation.

We specifically assessed the potential impact of dredging operations at five monitoring sites where signs of coral disease were reported. Four of these sites are reefs where the disease was observed by Precht et al. (2016) between Sept. and Dec. 2014. The fifth site is station HBSC1-CP, which was closely monitored throughout the expansion of PoM and where disease signs were already reported in May 2014 (Dial Cordy And Associates, 2017; Fig. 1A, see Appendix A). It remains however unclear if the disease observed at station HBSC1-CP was the SCTLD. The impact of dredging was assessed by identifying the dredging operations that produced sediment transported within 500 m of all five sites. We then computed the fraction of the sediment particles produced by these dredging operations that were actually transported within 500 m of the monitoring sites. The 500 m radius was chosen to match the scale of the 500 m × 500 m reef polygons used in the model (Dobbelaere et al., 2020). The resulting particle counts were then normalized by dividing them by the total number of sediment particles released by each dredging operation. Higher values of this indicator suggest a more significant impact of a specific type of dredging on the corresponding monitoring sites.

2.2. Wastewater backtracking

Additionally, we simulated the dispersal of pollutants backward in time from VKR and HBSC1-CP to identify sources of wastewater that could have affected these two sites. We chose this approach because other leaks than the one that was reported may be present along the pipe due to lack of maintenance (Staletovich, 2017b). Ten virtual particles – each representing a certain mass of dissolved pollutants – were released from each site every 450 s between September 26, 2014, and October 15, 2013, for a total of ~6.7×10^5 virtual particles per site. These simulations allowed us to assess whether wastewater leaking from the Miami Central District Municipal WWTP discharge pipe (Fig. 1B) could have impacted HBSC1-CP and VKR, as suggested by Gintert et al. (2019). As the leaking wastewater was initially reported by a fisherman (Staletovich, 2017b), we inferred that the majority of the wastewater particles possess positive buoyancy. However, certain wastewater constituents, such as fecal matter and heavy metals, exhibit negative buoyancy. These negatively buoyant components are likely to settle in close proximity to the source, resulting in limited dispersal. By focusing on positively buoyant particles, which are subject to transport by both currents and waves, we therefore modeled the worst-case scenario in which wastewater dispersal is maximized. The virtual pollutant particles were advected backward in time by a combination of ocean currents and Stokes drift from CMEMS' Ocean Wave Reanalysis dataset. We then computed risk maps by counting the number of particle trajectories intersecting each cell of a 200 m × 200 m grid, following the same approach as Anselain et al. (2023). This number was normalized by the total number of released particles to obtain the probability for each grid cell to be a source of pollution that would reach the monitoring sites.

This probability was then integrated along the wastewater discharge pipe, modeled as a straight line between Miami Central District Municipal WWTP, located on Virginia Key, and the ocean discharge outfall located at 25°44′31"N 80°05′10"W (Koopman et al., 2006).

2.3. Waterborne disease transmission

As previous studies showed evidence of waterborne transmission of SCTLD (Aeby et al., 2019; Dobbelaere et al., 2020; Eaton et al., 2021; Meiling et al., 2021), we assessed whether the disease could have been

[3] Datasets available at https://github.com/jrcunning/pom-dredge/

transmitted to VKR from other reefs affected by sediments from non-conventional dredging operations prior to September 2014. To evaluate this possibility, we computed monthly disease connectivity matrices following the methodology of Dobbelaere et al. (2020) during our simulated period. These connectivity matrices can be interpreted as large graphs whose vertices are 500 m × 500 m sub-reef polygons and whose edges represent disease connectivity pathways. Evaluating the possibility of disease propagation from sub-reefs affected by non-conventional dredging to VKR is therefore equivalent to evaluating the existence of pathways, *i.e.* sequences of connected vertices in the network starting from these sub-reefs and reaching VKR. As computing all possible pathways is not computationally tractable, we limited ourselves to the computation of shortest paths from the affected reefs to VKR. This was performed using the function get_all_shortest_paths of the Python python-igraph package (Csardi et al., 2006). Such a function requires the definition of a weight w_{ij} for the edge connecting reef i to reef j. We chose $w_{ij} = 1 - \widetilde{C}_{ij}$, where $\widetilde{C}_{ij}$ is the probability of disease propagation from reef i to reef j computed following the approach of Dobbelaere et al. (2020), so that 'shorter' edges of the networks (*i.e.* connectivity pathways with smaller weights) correspond to connections with a larger disease propagation probability. The probability of a given path was then defined as the mean connection probability of the edges composing this path.

3. Results

3.1. Sediment plume and deposition

We simulated sediment plumes for all dredging operations across five sediment size classes, with grain sizes ranging from 5 to 400 μm. Of these, only the grain sizes between 5 and 50 μm generated plumes that were consistent with the field data from satellite images reported by Barnes et al. (2015) and Cunning et al. (2019) (Fig. 2A). These plumes were most frequent between the coast and the reef line. For coarser grain sizes, particles settled closer to the dredged channel. The suspended sediments were then only observed offshore, closer to the Florida Current, where the current velocity was sufficiently strong to prevent deposition (Fig. 2B). This suggests that the observed turbidity was mostly due to fine silts. With grain sizes of 5–50 μm, the modeled occurrence of plumes within 15 km of the dredged matched the presence/absence data of Cunning et al. (2019) in 80.5 % of cases and the total area where plumes were observed was about 205 km^2, consistent with the ~228 km^2 estimated by Barnes et al. (2015). The simulated suspended sediment plumes mostly occurred north of the dredged channel, as particles were driven northward under the action of shelf currents influenced by winds and the Florida Current. The highest simulated plume frequency was about 60 % and was found within a region of about 1.5 km × 1.5 km north of the dredged channel and just next to Miami Beach (Fig. 2A). Plume frequencies locally reaching 30–40 % were observed within 4 km north of the dredged channel, between the coasts and the inner reef line. Suspended sediment plumes were observed during 0.32 % of simulated days at VKR site, 4.14 % at HBSC1-CP and 19.43 % at N. Sunny Isle. Similarly to Cunning et al. (2019), we found a positive correlation between plume frequency and sediment deposition, with a Pearson correlation coefficient of 0.29 (p-value $< 2.2 \times 10^{-16}$).

Deposition results are shown for grain sizes between 5 and 100 μm, corresponding to silts and very fine sand, which are more likely to carry organic matter and therefore more likely to carry SCTLD agents (Erftemeijer et al., 2012) (Fig. 2C,D). Sedimentation mostly occurred on reefs located north of the dredge channel, although some sediment particles deposited along the coastlines of Virginia Key, Key Biscayne and Miami for all modeled grain sizes. For grain sizes finer than 50 μm, sediments mostly settled on inshore reefs and along coastlines, while sedimentation mostly took place on offshore reefs for grain size coarser than 50 μm. Furthermore, sediment particles finer than 50 μm were deposited further south and west, covering the entire area between mainland Florida and the reef line. On average, the fraction of all sediments released depositing at VKR, HBSC1-CP and N. Sunny Isles was respectively 3.23×10^{-6} km^{-2}, 8.64×10^{-4} km^{-2} and 2.25×10^{-4} km^{-2} for grain sizes of 5–50 μm, and 7.63×10^{-6} km^{-2}, 1.39×10^{-3} km^{-2} and 5.72×10^{-4} km^{-2} for grain sizes of 50–100 μm. The deposition at these two sites therefore decreased with increasing grain sizes. Additionally, the fraction of the total particle mass depositing at Rainbow Reef and Emerald Reef was respectively 4.4×10^{-7} km^{-2} and 4.53×10^{-9} km^{-2} for grain sizes of 5–50 μm, while no sedimentation occurred at these sites for grain sizes of 50–100 μm.

Sediment particles with grain sizes of 5–50 μm and 50–100 μm, released by 99 % and 83 % of all simulated dredging operations respectively, reached N. Sunny Isles (Fig. 3). This makes it the reef site most impacted by the simulated dredging operations among the five sites considered here. HBSC1-CP was the second most impacted site, affected by 43 % and 35 % of the dredging operations involving grain sizes of 5–50 μm and 50–100 μm, respectively. VKR was the third most impacted site, receiving sediments from 12.4 % and 4.6 % of the dredging operations with grain sizes of 5–50 μm and 50–100 μm, respectively. Lastly, Rainbow Reef and Emerald Reef were each impacted by less than 4.5 % and 0.5 % of the dredging operations for grain sizes of 5–50 μm and 50–100 μm, respectively. More than 90 % of the modeled sediment particles were not transported within 500 m of the reef sites, and the proportion of particles reaching the monitoring sites decreased as grain sizes increased. Despite this, N. Sunny Isles, VKR, and HBSC1-CP were all affected by fine sediments from non-conventional dredging operations. Specifically, when considering these operations, VKR, HBSC1-CP, and N. Sunny Isles were impacted by 1.17 %, 4.37 %, and 14.80 % of the sediments released for grain sizes of 5–50 μm, respectively, and by 0.38 %, 2.19 %, and 3.36 % for grain sizes of 50–100 μm. However, since non-conventional dredging was expected to release more sediments into the water column than conventional one, where dredged material is collected, these relative metrics may underestimate the true impact of the non-conventional dredging operations.

3.2. Wastewater backtracking

When analyzing wastewater pollution by backtracking particle from HBSC1-CP and VKR, we see that the most likely sources of pollution impacting these sites were located within narrow "cones" directly south of the sites (see red parts of the plumes in Fig. 4). Within these cones, the probability of pollutants reaching the sites decreased southward: it fell below 30 % at a distance of 300 m, below 10 % between 1 and 1.5 km, below 5 % at 3 km, and below 1 % at 15 km from the sites. Outside these cones, the likelihood of pollutants reaching VKR and HBSC1-CP rapidly dropped below 1 %. The probability to be reached by particles originating from the leak reported by Staletovich (2017b) was 0 % for VKR and 1.6 % for HBSC1-CP. By integrating the probability of pollutant arrival along the wastewater discharge pipe, we found that less than 5 % of the pollutants leaking from the pipe would reach HBSC1-CP (located south of the pipe) if the leak is within 2 km. Beyond that distance, the fraction quickly drops below 1 % and become vanishingly small. For VKR, which is located north of pipe and hence downstream of this potential source of pollution, the fraction of pollutant impacting the site can reach 40 % but only within 500 m of the site. Beyond that distance, it quickly decreases below 1 % and vanishes.

3.3. Waterborne disease transmission

We then evaluated the likelihood that reefs affected by non-conventional dredging could become infected and subsequently transmit the disease to VKR. To do this, we calculated all the shortest paths from these impacted reefs to VKR using modeled monthly disease

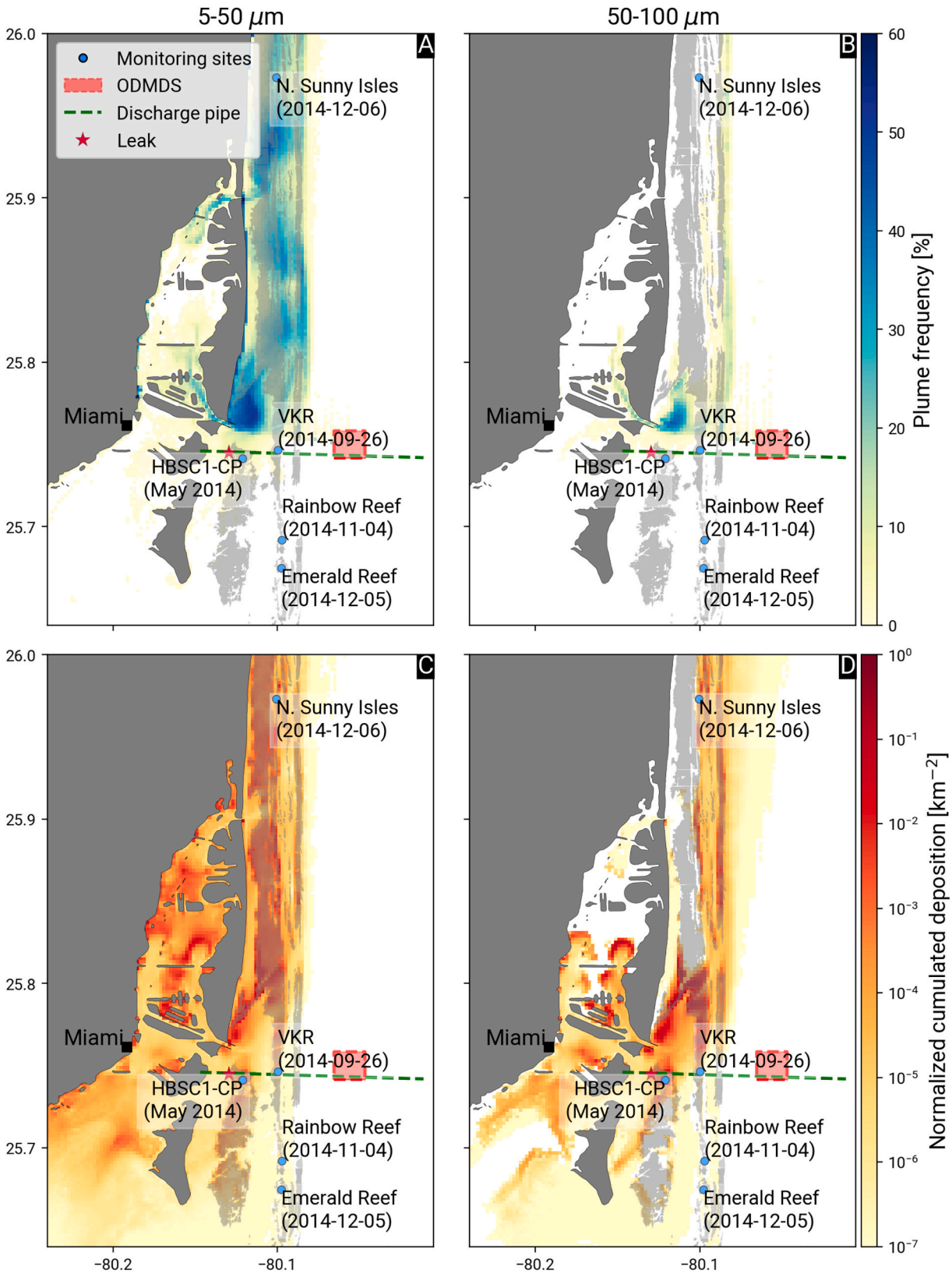

Fig. 2. Suspended sediment plume frequency for grain sizes in the range (A) 5–50 μm and (B) 50–100 μm. Averaged concentration of deposited sediments for grain sizes in the range (C) 5–50 μm and (D) 50–100 μm. The modeled turbidity and sedimentation mostly occurred north of the dredged channel.

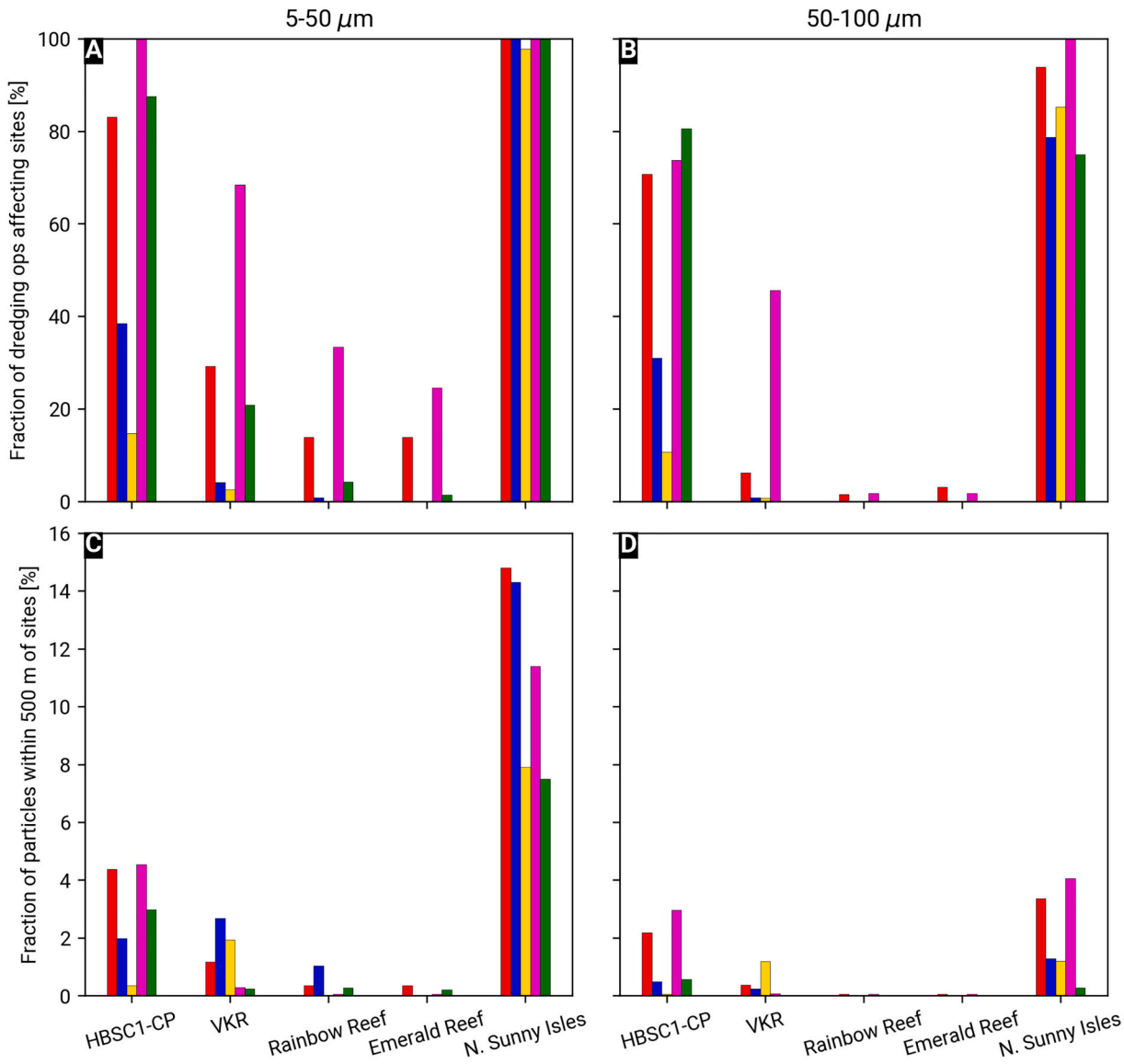

Fig. 3. Fraction of simulated dredging operations producing sediment particles that were transported within 500 m of HBSC1-CP, VKR and N. Sunny Isles for grain sizes of (A) 5–50 μm and (B) 50–100 μm. Fraction of the sediment particles produced by these operations transported within 500 m of HBSC1-CP, VKR and N. Sunny Isles for grain sizes of (C) 5–50 μm and (D) 50–100 μm. N. Sunny Isles was the most affected site. All sites were impacted by non-conventional dredging for the two considered grain sizes.

connectivity networks from May to September 2014 (Fig. 5). These reefs included HBSC1-CP, where potential signs of the disease were reported in May 2014. Our results reveal that there were connectivity pathways to VKR each month from May to September 2014, indicating a continuous potential for disease spread from the affected reefs to VKR during this period. Southern intermediary reefs were consistently needed as stepping stones for this disease transmission, suggesting that it might have taken several months for the disease agents to reach VKR from the reefs influenced by non-conventional dredging. However, the structure of these connectivity pathways remained relatively consistent throughout May-Sept. 2014, indicating persistent favorable conditions for disease propagation to VKR.

4. Discussion

Employing high-resolution ocean circulation and sediment transport models, we successfully reproduced sediment dynamics that align with plume observations from satellite imagery and *in situ* sediment deposition data at selected sites. The best agreement was obtained for grain sizes in the range 5–50 μm, suggesting that dredging operations mostly released fine-grained sediments, which include the very fine "rock flour" produced by non-conventional rock-chopping operations. Those sediments predominantly drifted northward, over several kilometers, under the influence of the Florida Current. The impact of dredging on southern sites such as Rainbow Reef and Emerald Reef was minimal, whereas up to 12 % of all dredging activities, and 29 % of the non-conventional ones, directly influenced VKR, where the initial outbreak of SCTLD was reported in September 2014 (Precht et al., 2016). Additionally, our analysis suggests that the VKR site was unlikely to be affected by wastewater leaking from the Miami Central District Municipal WWTP discharge pipe unless the leakage occurred within 500 m of the site. Notably, signs of a disease – though not definitively identified as SCTLD – were observed at HBSC1-CP prior to September 2014, coinciding with both sediment plumes and deposition documented in our simulations. Moreover, monthly disease connectivity networks revealed that disease agents could have spread from reefs affected by non-conventional dredging to VKR *via* multistep connectivity pathways.

Our study confirms previous findings on the extensive impacts of the

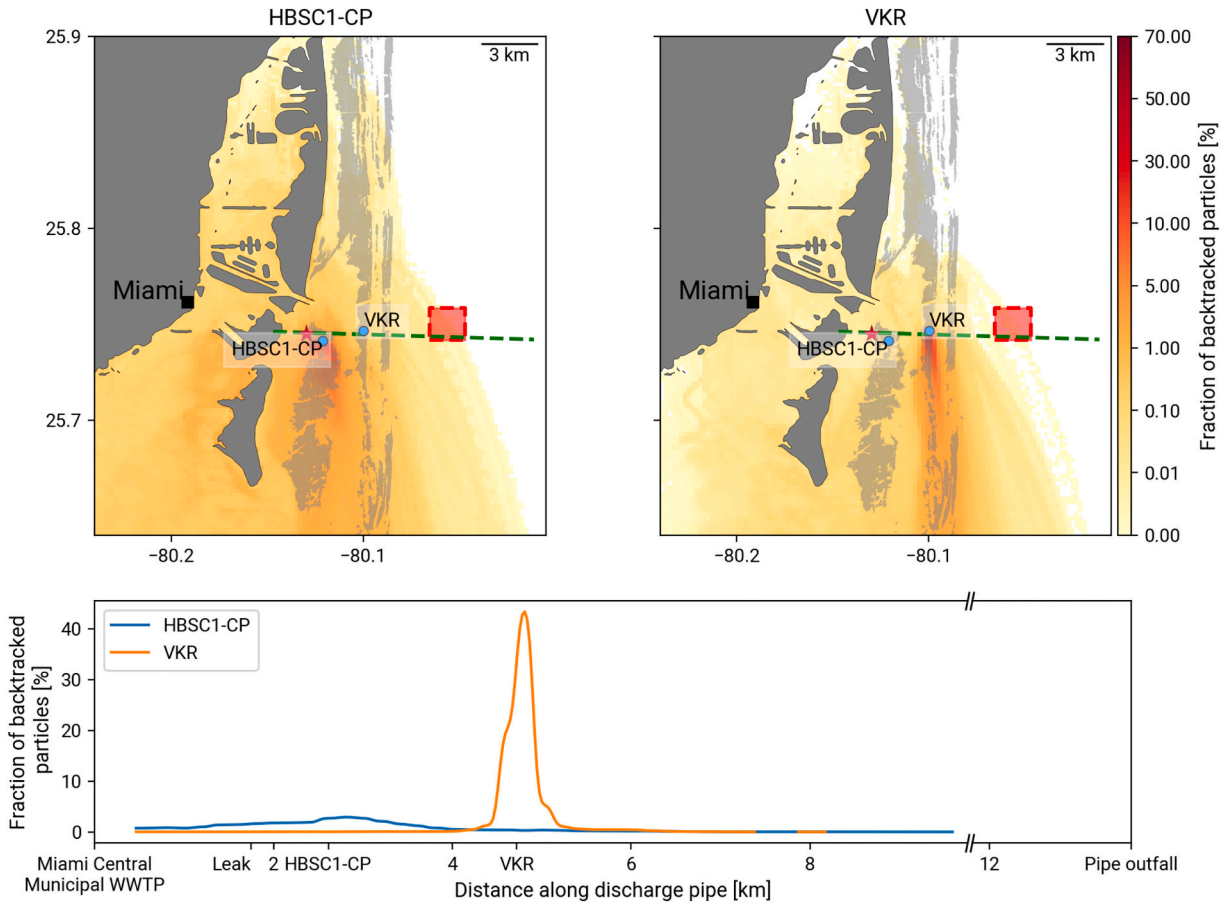

Fig. 4. Spatial distribution of the probability to be a source of positively buoyant pollutants reaching HBSC1-CP (top left) and VKR (top right). Bottom: Integration of this probability along the discharge pipe of Miami Central District Municipal WWTP, which was reported to leak in 2017. Most likely sources of pollutants were located within a few kilometers south of HBSC1-CP and VKR. In the top panels, the Ocean Dredge Material Disposal Site (ODMDS) is shown in red and the discharge pipe of the Miami Central Municipal WWTP in green. (For interpretation of the references to colour in this figure legend, the reader is referred to the web version of this article.)

PoM expansion. Echoing Barnes et al. (2015), the sediment plumes simulated with our model have a total surface area of about 205 km^2. Additionally, our model achieved an 80.5 % accuracy in replicating the presence or absence of plumes within 15 km of the dredged channel, as detailed by Cunning et al. (2019). This high level of accuracy was specifically observed for grain sizes ranging from 5 to 50 μm. This suggests that the silt and clay-like "rock flour" materials, resulting from unconventional rock chopping, were the primary contributors to the turbidity during dredging, aligning with findings from previous research (Storlazzi et al., 2015; Fourney and Figueiredo, 2017). Despite this congruence, our model predicted a northward shift in plume distribution compared to these earlier studies, possibly due to our method focusing solely on suspended sediment concentration, whereas turbidity is influenced by various local factors including phytoplankton water content and organic matter (Gray, 2000; Thackston and Palermo, 2000). Consistent with Cunning et al. (2019), our results identified a positive correlation between sedimentation rates and plume frequency. Significantly, the regions with the highest cumulative sediment deposition were predominantly over coral reefs, suggesting that the PoM expansion adversely affected coral populations across a broad area through increased turbidity and sedimentation. The sediment primarily settled on nearshore reefs with finer grain sizes and on offshore reefs with coarser grains. This sedimentation could be particularly detrimental to offshore coral reef populations, which are generally less adapted to sediment exposure compared to their inshore counterparts (Wolanski et al., 2005). Furthermore, Long et al. (2002) found that fine sediments in the vicinity of the Miami River and in the PoM could accumulate significant levels of heavy metals.

A limitation of our study is that conventional and non-conventional dredging operations are treated in the same way in the model. For all dredging types, sediment particles were released at the same rate. Although conventional dredging was reported to release fine-grained sediments in the water column through dewatering and barge overflow (Jones et al., 2016), the quantity of dredged material lost in the water was limited by the use of pumping mechanisms. In contrast, for non-conventional dredging, the suction mechanism was turned off, causing all chopped rock particles to be released in the water column. The numbers of particles reaching the monitoring sites were therefore likely underestimated for non-conventional dredging operations. However, the fractions given in Fig. 3C,D remain valid as they are relative to the total amount of sediment released in the water column for each type of dredging operation. When considering the simulated sediment plumes with the finest grain sizes, VKR, HBSC1-CP and N. Sunny Isles were respectively affected by 29 %, 83 % and 100 % of the non-conventional dredging operations that took place between December 2013 and May 2014. Furthermore, HBSC1-CP exhibited the highest deposition of sediments produced by non-conventional dredging. These sediment particles therefore had a higher probability to settle and to be in direct contact with corals. In addition to smothering corals and diverting their energy through sediment removal (Erftemeijer et al., 2012), these settled sediments spend more time in direct contact with the corals and might therefore yield a stronger disease transmission potential.

Our sediment simulations indicate that up to 29 % of non-conventional dredging operations directly impacted VKR, where the

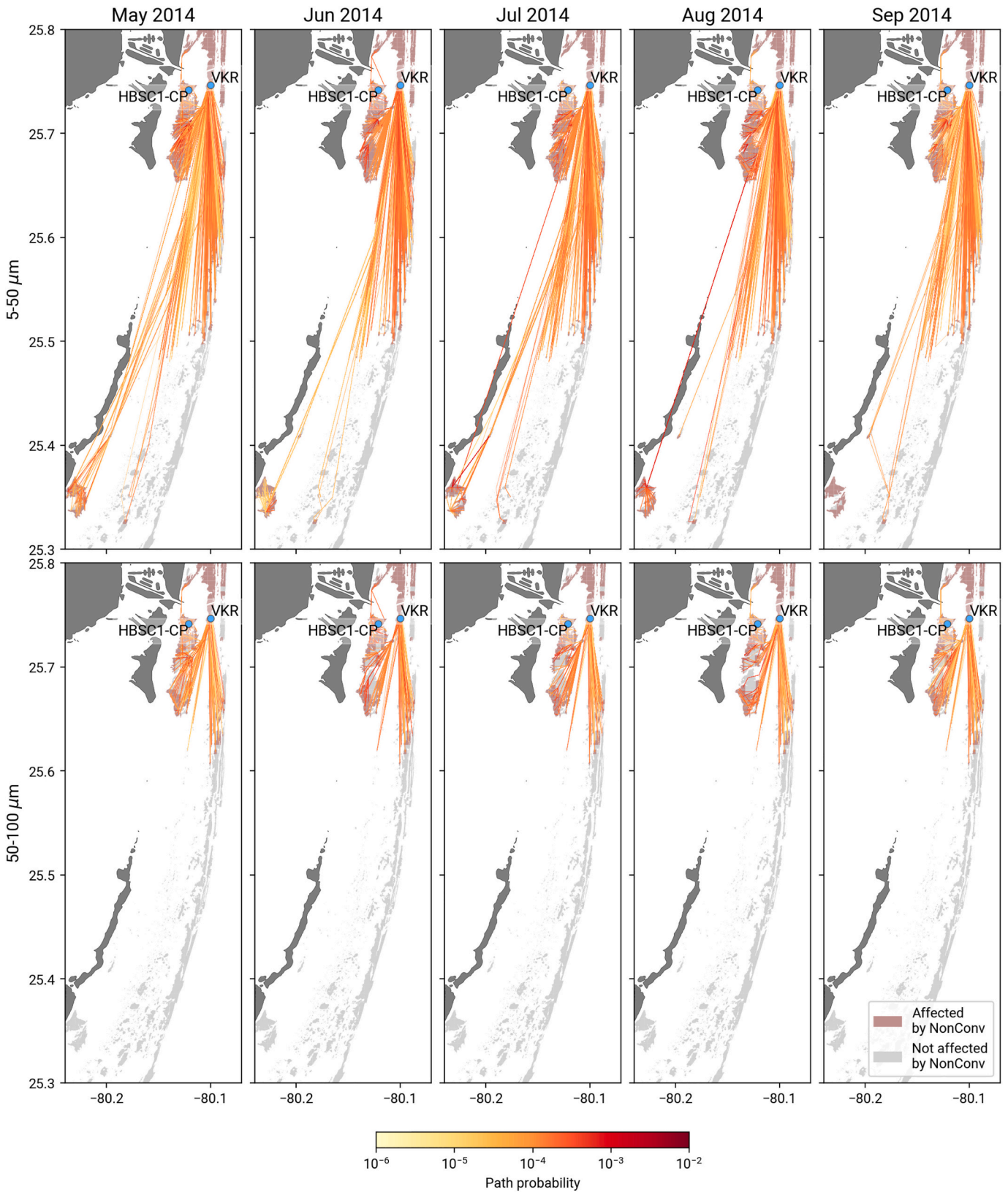

Fig. 5. Shortest path distributions from all the reefs affected by non-conventional dredging operations to the monitoring site near Virginia Key (VKR) for the monthly disease connectivity networks of May to September 2014. Southern intermediary reefs were always needed as stepping stones for the propagation of the disease to VKR.

outbreak was first reported in September 2014 (Precht et al., 2016). Additionally, backtracking of positively buoyant pollutants from VKR showed that the likelihood of reaching the site quickly dropped below 1 % for sources not directly south of VKR. An analysis along the Miami Central District Municipal WWTP discharge pipe suggested that contamination by leaking wastewater was improbable unless the leak was within a few hundred meters of VKR. These results are consistent with the trajectories of drifters released at the location of the leak (Staletovich, 2017a). Moreover, reports of a leaking pipe only emerged in 2017 (Staletovich, 2017b), with no prior evidence of leakage before September 2014. Despite this, signs of disease were observed before September 2014 at HBSC1-CP, a site significantly affected by non-conventional dredging. While these signs were not definitively identified as SCTLD, we did not dismiss the possibility and explored the potential for waterborne transmission from all reefs affected by non-conventional dredging to VKR. Our construction and analysis of monthly disease connectivity networks from May to September 2014 revealed potential for multiple disease pathways from those affected reefs to VKR. All these pathways required southern reefs as intermediary steps. Given an average transmission time of 5–10 days (Dobbelaere et al., 2020), the disease could have taken several months to reach VKR, aligning with the observed 5-month interval between reports at the two sites. The consistency of connectivity pathways throughout this period further supports the possibility of uninterrupted disease propagation due to stable hydrodynamic conditions.

Our study shows that dredging operations can have a large environmental footprint that exceeds the direct vicinity of the dredged area. That is even more the case when large amounts of fine-grained sediments are extracted and released in the water column. While the initial Environmental Impact Statement (EIS) concluded that the PoM dredging would result in about 13,350 m^2 of reef that would be permanently removed by dredging (U.S. Army Corps of Engineers, 2004), it finally appeared that 1.125 km^2 of coral reef had been lost (NOAA's National Marine Fisheries Service, 2023) and much more if we account for the possibility that it triggered the SCTLD epidemic. The reef site where SCTLD was first identified in Sept. 2014 was not supposed to be impacted by dredging operations. Our results nonetheless suggest that it had been impacted by fine sediments resulting from non-conventional dredging prior to the disease onset. These operations were neither planned nor authorised in the EIS. While we did not consider all possible contamination mechanisms (*e.g.* hull fouling) and can hence not definitively assert with complete certainty that these operations were responsible for the onset of the disease at VKR, we could nonetheless identify a clear physical connection between these two events.

Our model results suggest that either directly or indirectly, through disease transmission from intermediary reefs, the dredging of the PoM - and more specifically the non-conventional rock-chopping operations - had the potential to deliver disease agents to the reefs suspected to have experienced the first SCTLD outbreaks. If the etiological agent of SCTLD were present in or associated with the those sediments, these operations could be implicated in the onset of one of the most severe and damaging coral disease epidemics to date. While we may never fully ascertain this transmission pathway, our results emphasize the need for greater caution in future large-scale dredging projects to minimize environmental impacts, particularly on coral reefs already heavily stressed by recent bleaching events and poor water quality. Effective strategies should include enforcing stricter operational guidelines to eliminate rock-chopping, limiting the dispersion of fine sediments, implementing real-time monitoring of sediment plumes, adapting dredging operations to current and wave forecasts, and using silt curtains extensively to safeguard sensitive marine ecosystems. Additionally, our results suggest that wastewater discharge pipes should be more carefully monitored and maintained in sections close to sensitive habitats. It is encouraging to note that some of these measures are being incorporated into ongoing and planned port expansions in southeast Florida, such as Phase IV of Port Miami and the Port Everglades expansion, located about 37 km north of Port Miami (NOAA's National Marine Fisheries Service, 2023).

CRediT authorship contribution statement

Thomas Dobbelaere: Writing – review & editing, Writing – original draft, Validation, Methodology, Investigation. **Daniel M. Holstein:** Writing – review & editing, Conceptualization. **Lewis J. Gramer:** Writing – review & editing, Conceptualization. **Lucas McEachron:** Writing – review & editing, Conceptualization. **Emmanuel Hanert:** Writing – review & editing, Supervision, Conceptualization.

Declaration of competing interest

The authors declare that they have no known competing financial interests or personal relationships that could have appeared to influence the work reported in this paper.

Data availability

Data will be made available on request.

Acknowledgments

Computational resources were provided by the Consortium des Équipements de Calcul Intensif (CéCI), funded by the F.R.S.-FNRS under Grant No. 2.5020.11. Thomas Dobbelaere is a Postdoctoral Researcher supported by the F.R.S.-FNRS. We are grateful to Jocelyn Karazsia and Xaymara Serrano for their comments and assistance in analyzing the data and reports related to the expansion of the Port of Miami.

Appendix A. Reported disease signs at site HBSC1-CP in May 2014

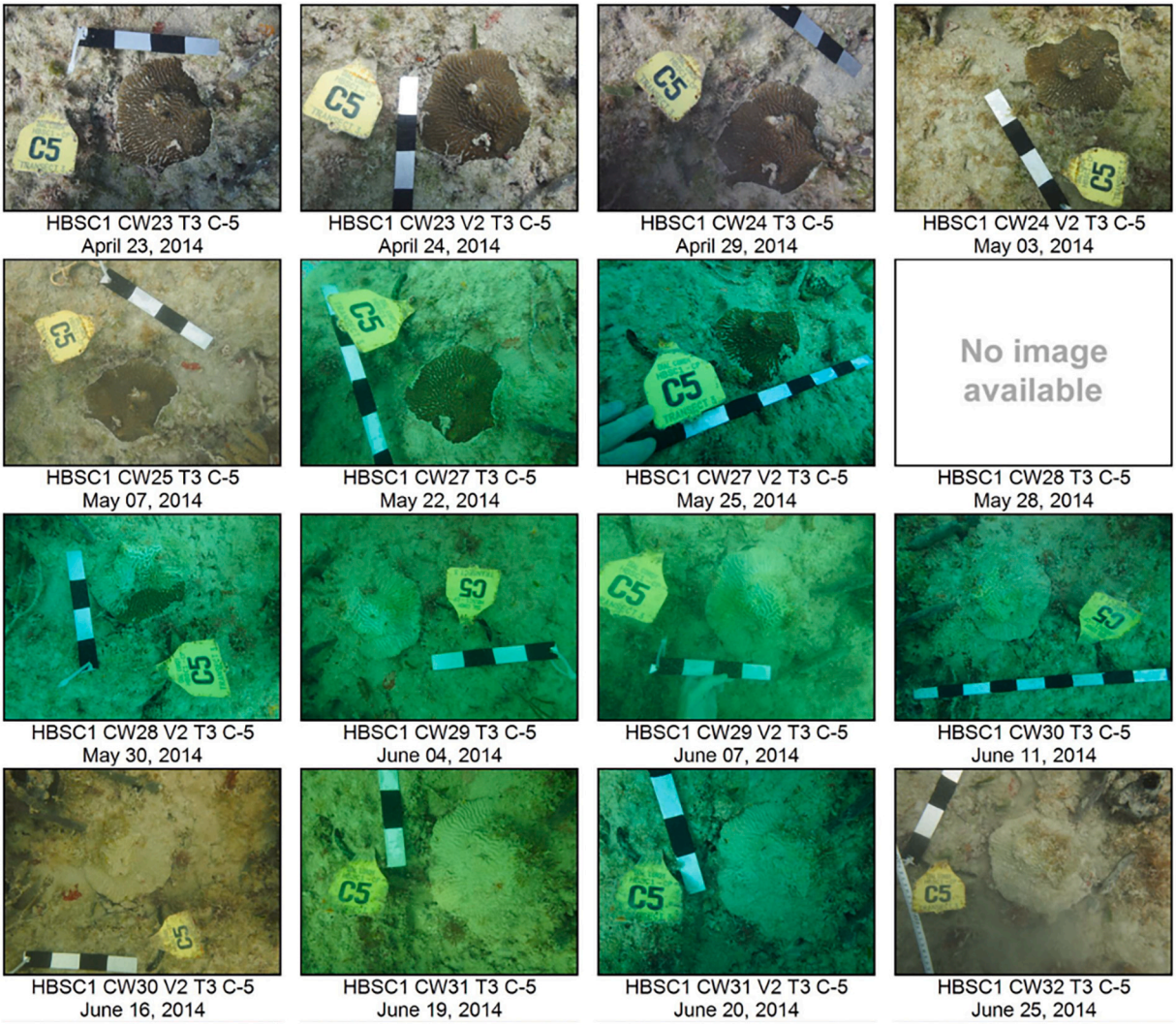

Fig. A.6. Lightroom photos of tagged corals at site HBSC1-CP (Dial Cordy And Associates, 2017). The first signs of the disease appeared between May 25 and May 30. By June 4, the whole colony was completely dead

Appendix B. Model validation against tide gauge observations

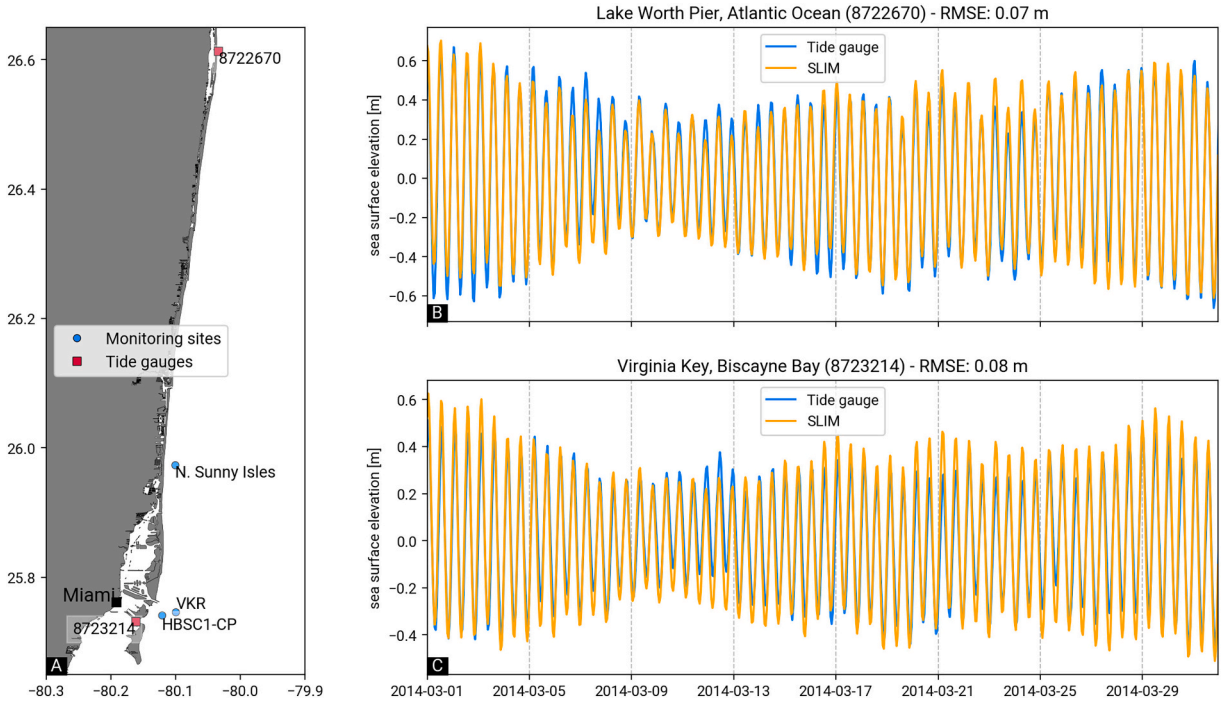

Fig. B.7. (A) Locations of the tide gauge stations (width IDs 8722670 and 8723214) from the National Data Buoy Center used to validated the modeled hydrodynamics. (B)-(C) Comparison of the modeled sea surface elevation against tide gauge measurements in March 2014. The model Root Mean Square Error (RMSE) was below 10 cm at both stations.

References

Aeby, G., Ushijima, B., Campbell, J.E., Jones, S., Williams, G., Meyer, J.L., Hase, C., Paul, V., 2019. Pathogenesis of a tissue loss disease affecting multiple species of corals along the Florida Reef Tract. Front. Mar. Sci. 6, 678.

Anselain, T., Heggy, E., Dobbelaere, T., Hanert, E., 2023. Qatar Peninsula's vulnerability to oil spills and its implications for the global gas supply. Nature Sustain. 6, 273–283.

Anthony, K.R., 1999. A tank system for studying benthic aquatic organisms at predictable levels of turbidity and sedimentation: case study examining coral growth. Limnol. Oceanogr. 44, 1415–1422.

Aronson, R.B., Precht, W.F., 2001. White-band disease and the changing face of Caribbean coral reefs. In: The Ecology and Etiology of Newly Emerging Marine Diseases. Springer, pp. 25–38.

Barnes, B.B., Hu, C., Kovach, C., Silverstein, R.N., 2015. Sediment plumes induced by the port of Miami dredging: analysis and interpretation using Landsat and MODIS data. Remote Sens. Environ. 170, 328–339.

Brandt, M.E., McManus, J.W., 2009. Dynamics and impact of the coral disease white plague: insights from a simulation model. Dis. Aquat. Org. 87, 117–133.

Breivik, Ø., Bidlot, J.R., Janssen, P.A., 2016. A stokes drift approximation based on the Phillips spectrum. Ocean Model 100, 49–56.

Chassignet, E.P., Hurlburt, H.E., Smedstad, O.M., Halliwell, G.R., Hogan, P.J., Wallcraft, A.J., Baraille, R., Bleck, R., 2007. The HYCOM (hybrid coordinate ocean model) data assimilative system. J. Mar. Syst. 65, 60–83.

Csardi, G., Nepusz, T., et al., 2006. The igraph software package for complex network research. InterJournal, complex systems 1695, 1–9.

Cunning, R., Silverstein, R.N., Barnes, B.B., Baker, A.C., 2019. Extensive coral mortality and critical habitat loss following dredging and their association with remotely-sensed sediment plumes. Mar. Pollut. Bull. 145, 185–199.

Dial Cordy And Associates, 2017. Miami Harbor Phase III Federal Channel Expansion Project Permit No. 030572-001-BI: One-Year Post-Construction Impact Assessment for Hardbottom Middle and Outer Reef Benthic Communities at Permanent Sites. Appendix B: LIGHTROOM PHOTOS OF TAGGED CORALS BASELINE THROUGH IMPACT ASSESSMENT.

Dobbelaere, T., Muller, E.M., Gramer, L.J., Holstein, D.M., Hanert, E., 2020. Coupled epidemio-hydrodynamic modeling to understand the spread of a deadly coral disease in Florida. Front. Mar. Sci. 7, 1016.

Dobbelaere, T., Curcic, M., Le Hénaff, M., Hanert, E., 2022a. Impacts of hurricane Irma (2017) on wave-induced ocean transport processes. Ocean Model 101947. https://doi.org/10.1016/j.ocemod.2022.101947.

Dobbelaere, T., Holstein, D.M., Muller, E.M., Gramer, L.J., McEachron, L., Williams, S.D., Hanert, E., 2022b. Connecting the dots: transmission of stony coral tissue loss disease from the Marquesas to the Dry Tortugas. Front. Mar. Sci. https://doi.org/10.3389/fmars.2022.778938.

E.U. Copernicus Marine Service Information (CMEMS), 1993–2021. Global Ocean Waves Reanalysis. https://doi.org/10.48670/moi-00022.

Eaton, K.R., Landsberg, J.H., Kiryu, Y., Peters, E.C., Muller, E.M., 2021. Measuring stony coral tissue loss disease induction and lesion progression within two intermediately susceptible species. Montastraea cavernosa and Orbicella faveolata. Front. Mar. Sci. 1287.

Eddy, T.D., Lam, V.W.Y., Reygondeau, G., Cisneros-Montemayor, A.M., Greer, K., Palomares, M.L.D., Bruno, J.F., Ota, Y., Cheung, W.W.L., 2021. Global decline in capacity of coral reefs to provide ecosystem services. One Earth 4, 1278–1285. https://doi.org/10.1016/j.oneear.2021.08.016.

Elliff, C.I., Silva, I.R., 2017. Coral reefs as the first line of defense: shoreline protection in face of climate change. Mar. Environ. Res. 127, 148–154. https://doi.org/10.1016/j.marenvres.2017.03.007.

Erftemeijer, P.L., Riegl, B., Hoeksema, B.W., Todd, P.A., 2012. Environmental impacts of dredging and other sediment disturbances on corals: a review. Mar. Pollut. Bull. 64, 1737–1765.

Estrada-Saldívar, N., Quiroga-García, B.A., Pérez-Cervantes, E., Rivera-Garibay, O.O., Alvarez-Filip, L., 2021. Effects of the stony coral tissue loss disease outbreak on coral communities and the benthic composition of Cozumel reefs. Front. Mar. Sci. 8, 306.

Fabricius, K.E., 2005. Effects of terrestrial runoff on the ecology of corals and coral reefs: review and synthesis. Mar. Pollut. Bull. 50, 125–146.

Ferrario, F., Beck, M., Storlazzi, C., Micheli, F., Shepard, C., Airoldi, L., 2014. The effectiveness of coral reefs for coastal hazard risk reduction and adaptation. Nat. Commun. 5, 3794. https://doi.org/10.1038/ncomms4794.

Fourney, F., Figueiredo, J., 2017. Additive negative effects of anthropogenic sedimentation and warming on the survival of coral recruits. Sci. Rep. 7, 1–8.

Frys, C., Saint-Amand, A., Le Hénaff, M., Figueiredo, J., Kuba, A., Walker, B., Lambrechts, J., Vallaeys, V., Vincent, D., Hanert, E., 2020. Fine-scale coral connectivity pathways in the Florida reef tract: implications for conservation and restoration. Front. Mar. Sci. 7, 312.

Geuzaine, C., Remacle, J.F., 2009. Gmsh: a 3-D finite element mesh generator with built-in pre-and post-processing facilities. Int. J. Numer. Methods Eng. 79, 1309–1331.

Gintert, B.E., Precht, W.F., Fura, R., Rogers, K., Rice, M., Precht, L.L., D'Alessandro, M., Croop, J., Vilmar, C., Robbart, M.L., 2019. Regional coral disease outbreak overwhelms impacts from a local dredge project. Environ. Monit. Assess. 191, 1–39.

Gray, J.R., 2000. Comparability of suspended-sediment concentration and total suspended solids data. In: 4191, US Department of the Interior. Survey, US Geological.

Hamilton, E.L., Bachman, R.T., 1982. Sound velocity and related properties of marine sediments. J. Acoust. Soc. Am. 72, 1891–1904.

Harvell, D., Jordán-Dahlgren, E., Merkel, S., Rosenberg, E., Raymundo, L., Smith, G., Weil, E., Willis, B., 2007. Coral disease, environmental drivers, and the balance between coral and microbial associates. Oceanography 20, 172–195.

Hennige, S.J., Smith, D.J., Perkins, R., Consalvey, M., Paterson, D.M., Suggett, D.J., 2008. Photoacclimation, growth and distribution of massive coral species in clear and turbid waters. Mar. Ecol. Prog. Ser. 369, 77–88.

Heres, M.M., Farmer, B.H., Elmer, F., Hertler, H., 2021. Ecological consequences of stony coral tissue loss disease in the Turks and Caicos Islands. Coral Reefs 40, 609–624.
Jones, R., Ricardo, G., Negri, A., 2015. Effects of sediments on the reproductive cycle of corals. Mar. Pollut. Bull. 100, 13–33.
Jones, R., Bessell-Browne, P., Fisher, R., Klonowski, W., Slivkoff, M., 2016. Assessing the impacts of sediments from dredging on corals. Mar. Pollut. Bull. 102, 9–29.
Jones, R., Fisher, R., Bessell-Browne, P., 2019. Sediment deposition and coral smothering. PLoS One 14, e0216248.
Kendall Jr., J., Powell, E., Connor, S., Bright, T., 1983. The effects of drilling fluids (muds) and turbidity on the growth and metabolic state of the coral acropora cervicornis, with comments on methods of normalization for coral data. Bull. Mar. Sci. 33, 336–352.
Koopman, B., Heaney, J.P., Cakir, F.Y., Rembold, M., Indeglia, P., Kini, G., 2006. Ocean Outfall Study. Florida Department of Environmental Protection, Tallahassee.
Kramer, P., Roth, L., Lang, J., 2019. Map of stony coral tissue loss disease outbreak in the Caribbean. URL. www.agrra.org.
Long, E.R., Hameedi, M.J., Sloane, G.M., Read, L.B., 2002. Chemical contamination, toxicity, and benthic community indices in sediments of the lower Miami river and adjoining portions of Biscayne Bay, Florida. Estuaries 25, 622–637.
MacDonald, N.J., Davies, M.H., Zundel, A.K., Howlett, J.D., Demirbilek, Z., Gailani, J.Z., Lackey, T.C., Smith, J., 2006. PTM: Particle Tracking Model. Report 1: Model Theory, Implementation, and Example Applications. Technical Report.. Engineer Research And Development Center Vicksburg MS Coastal And Hydraulics Lab.
Meiling, S.S., Muller, E.M., Lasseigne, D., Rossin, A., Veglia, A.J., MacKnight, N., Dimos, B., Huntley, N., Correa, A., Smith, T.B., et al., 2021. Variable species responses to experimental stony coral tissue loss disease (SCTLD) exposure. Front. Mar. Sci. 8, 464.
Moberg, F., Folke, C., 1999. Ecological goods and services of coral reef ecosystems. Ecol. Econ. 29, 215–233. https://www.sciencedirect.com/science/article/pii/S0921800999000099. https://doi.org/10.1016/S0921-8009(99)00009-9.
Muller, E.M., Sartor, C., Alcaraz, N.I., van Woesik, R., 2020. Spatial epidemiology of the stony-coral-tissue-loss disease in Florida. Front. Mar. Sci. 7, 163.
NOAA''s National Marine Fisheries Service, 2023. Examination of sedimentation impacts to coral reef along the port miami entrance channel, december 2015 and april 2016. URL. https://www.ncei.noaa.gov/data/oceans/coris/library/NOAA/CRCP/NMFS/SERO/Projects/30049/Karazsia2023_PortMiami_Dredge_PhaseIII_ImpactAssessment_FinalReport.pdf (Accessed on August 4).
Pollock, F.J., Lamb, J.B., Field, S.N., Heron, S.F., Schaffelke, B., Shedrawi, G., Bourne, D.G., Willis, B.L., 2014. Sediment and turbidity associated with offshore dredging increase coral disease prevalence on nearby reefs. PLoS One 9, e102498.
Precht, W.F., Gintert, B.E., Robbart, M.L., Fura, R., Van Woesik, R., 2016. Unprecedented disease-related coral mortality in southeastern Florida. Sci. Rep. 6, 1–11.
Richardson, L.L., Goldberg, W.M., Carlton, R.G., Halas, J.C., 1998. Coral disease outbreak in the Florida keys: plague type II. Rev. Biol. Trop. 187–198.
Rogers, A., Blanchard, J.L., Mumby, P.J., 2014. Vulnerability of coral reef fisheries to a loss of structural complexity. Curr. Biol. 24, 1000–1005. https://doi.org/10.1016/j.cub.2014.03.026.
Rogers, C.S., 1990. Responses of coral reefs and reef organisms to sedimentation. Marine ecology progress series. Oldendorf 62, 185–202.
Rosales, S.M., Sinigalliano, C., Gidley, M., Jones, P.R., Gramer, L.J., 2019. Oceanographic habitat and the coral microbiomes of urban-impacted reefs. PeerJ 7, e7552.
Rosales, S.M., Clark, A.S., Huebner, L.K., Ruzicka, R.R., Muller, E., 2020. Rhodobacterales and Rhizobiales are associated with stony coral tissue loss disease and its suspected sources of transmission. Front. Microbiol. 11, 681.
Saint-Amand, A., Grech, A., Choukroun, S., Hanert, E., 2022. Quantifying the environmental impact of a major coal mine project on the adjacent great barrier reef ecosystems. Mar. Pollut. Bull. 179, 113656.
Soulsby, R., Whitehouse, R., et al., 1997. Threshold of sediment motion in coastal environments, in: Pacific Coasts and Ports'97. Proceedings, pp. 149–154.
Spadafore, R., Fura, R., Precht, W.F., Vollmer, S.V., 2021. Multi-variate analyses of coral mortality from the 2014–2015 stony coral tissue loss disease outbreak off Miami-Dade County. Florida. Front. Mar. Sci. 8, 723998.
Spalding, M.D., Grenfell, A.M., 1997. New estimates of global and regional coral reef areas. Coral Reefs 16, 225–230. https://doi.org/10.1007/s003380050078.
Staletovich, J., 2017a. Miami Sewage Leak didn't Stay at Sea; it Flowed toward Wildlife Preserve, Ritzy Residences. URL. https://www.miamiherald.com/news/local/environment/article166801597.html.
Staletovich, J., 2017b. Miami's Sewage Is Supposed to Be Pumped Offshore but the Pipe Has Sprung a Leak. URL. https://www.miamiherald.com/news/local/environment/article164655777.html.
Storlazzi, C.D., Norris, B.K., Rosenberger, K.J., 2015. The influence of grain size, grain color, and suspended-sediment concentration on light attenuation: why fine-grained terrestrial sediment is bad for coral reef ecosystems. Coral Reefs 34, 967–975.
Studivan, M.S., Rossin, A.M., Rubin, E., Soderberg, N., Holstein, D.M., Enochs, I.C., 2022. Reef sediments can act as a stony coral tissue loss disease vector. Front. Mar. Sci. 2046.
Sutherland, K.P., Porter, J.W., Torres, C., 2004. Disease and immunity in Caribbean and indo-Pacific zooxanthellate corals. Mar. Ecol. Prog. Ser. 266, 273–302.
Thackston, E., Palermo, M.R., 2000. Improved Methods for Correlating Turbidity and Suspended Solids for Monitoring. US Army Engineer Research and Development Center.
U.S. Army Corps of Engineers, 2004. Final Environmental Impact Statement for the Miami Harbor. Technical Report, URL. https://www.saj.usace.army.mil/About/Divisions-Offices/Planning/Environmental-Branch/Environmental-Documents/ (Accessed April 11, 2024).
U.S. Army Corps of Engineers, 2023. Final environmental assessment : Maintenance dredging and dredged material placement for Miami Harbor navigation project at port Miami in Miami-Dade County, Florida. In: Appendix D: Other Reports and Related Documents. Report. URL, Technical. https://www.saj.usace.army.mil/About/Divisions-Offices/Planning/Environmental-Branch/Environmental-Documents/ (Accessed August 7, 2024).
Weber, M., De Beer, D., Lott, C., Polerecky, L., Kohls, K., Abed, R.M., Ferdelman, T.G., Fabricius, K.E., 2012. Mechanisms of damage to corals exposed to sedimentation. Proc. Natl. Acad. Sci. 109, E1558–E1567.
Wittenberg, M., Hunte, W., 1992. Effects of eutrophication and sedimentation on juvenile corals. Mar. Biol. 112, 131–138.
Wolanski, E., Fabricius, K., Spagnol, S., Brinkman, R., 2005. Fine sediment budget on an inner-shelf coral-fringed island, great barrier reef of Australia. Estuar. Coast. Shelf Sci. 65, 153–158.